Electronic Supplementary Material (ESI) for Physical Chemistry Chemical Physics.
This journal is © the Owner Societies 2021

**Electronic Supplementary Information for:**

# Twisted Bodipy Derivative: Intersystem Crossing, Electron Spin Polarization and Application as a Novel Photodynamic Therapy Reagent

Yu Dong, ‡[a] Prashant Kumar,‡[b] Partha Maity,‡[c] Ivan Kurganskii,[d] Shujing Li,[e] Ayhan Elmali,[f] Jianzhang Zhao,*[a] Daniel Escudero,*[b] Huijian Wu,*[e] Ahmet Karatay,*[f] Omar F. Mohammed*[c] and Matvey Fedin*[d]

[a] State Key Laboratory of Fine Chemicals, School of Chemical Engineering, Dalian University of Technology, E-208 West Campus, 2 Ling Gong Road, Dalian 116024, P. R. China. E-mail: zhaojzh@dlut.edu.cn

[b] Department of Chemistry, KU Leuven, Celestijnenlaan 200F, B-3001 Leuven, Belgium. Email: Daniel.escudero@kuleuven.be

[c] Division of Physical Sciences and Engineering, King Abdullah University of Science and Technology (KAUST), Thuwal 23955-6900, Kingdom of Saudi Arabia. Email: omar.abdelsaboor@kaust.edu.sa

[d] International Tomography Center, SB RAS Institutskaya Str., 3A, and Novosibirsk State University, Pirogova str. 2, 630090 Novosibirsk, Russia. Email: mfedin@tomo.nsc.ru

[e] School of Life Science and Biotechnology, Dalian University of Technology, Dalian 116024, P. R. China. E-mail: wuhj@dlut.edu.cn

[f] Department of Chemistry, Faculty of Science, and Department of Engineering Physics, Faculty of Engineering, Ankara University, 06100 Beşevler, Ankara, Turkey. Email: Ahmet.Karatay@eng.ankara.edu.tr

‡ These authors contributed equally to this work.

## Table of Contents

**1.0 UV-Vis Absorption and Fluorescence Spectra.**

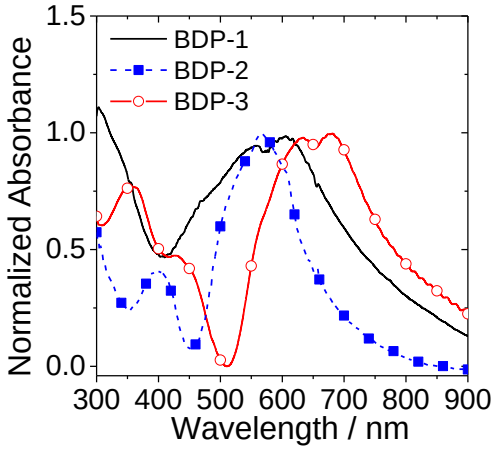


**Fig. S1** Normalized absorption of **BDP-1**, **BDP-2** and **BDP-3** in film (Clear Flex 50® film) prepared by evaporating solvent of DCM solution of compounds. 20 °C.

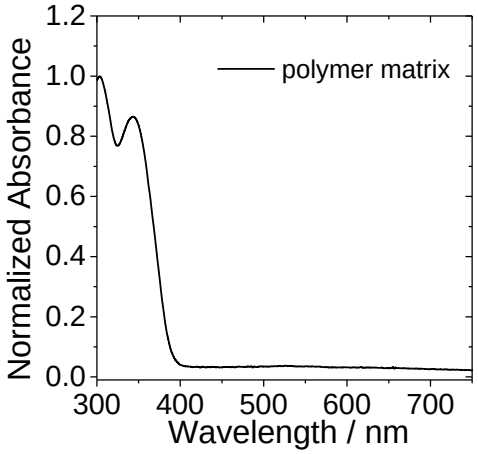


**Fig. S2** Normalized absorption of polymer matrix film (Clear Flex 50® film) alone prepared by evaporating solvent of DCM solution. 20 °C.

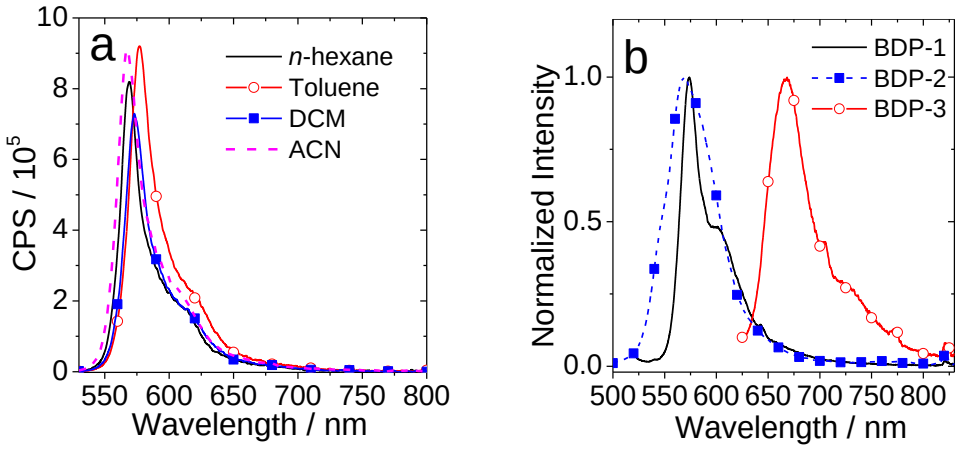


**Fig. S3** Fluorescence emission spectra and of (a) **BDP-1** in different solvents. Optically matched solutions were used. $A = 0.142$, $\lambda_{ex} = 520$ nm. (b) Normalized fluorescence emission spectra of **BDP-1**, **BDP-2** and **BDP-3** in Clear Flex 50® film. 20 °C.

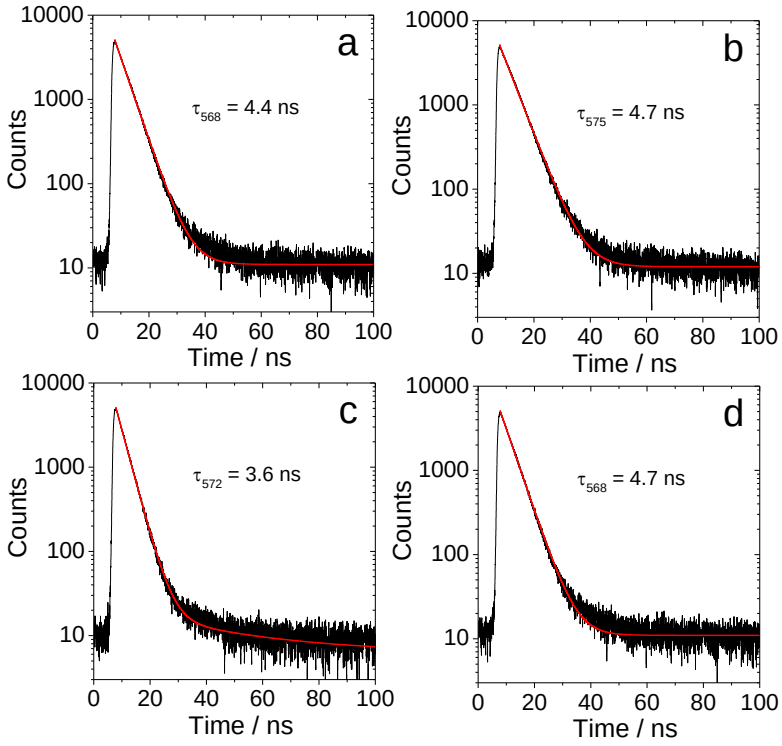


**Fig. S4** Fluorescence decay curves of **BDP-1** (a) In *n*-hexane, (b) In toluene, (c) In DCM and (d) In ACN. $c$ =1.0 × $10^{-5}$ M, $\lambda_{ex} = 510$ nm. 20 °C.

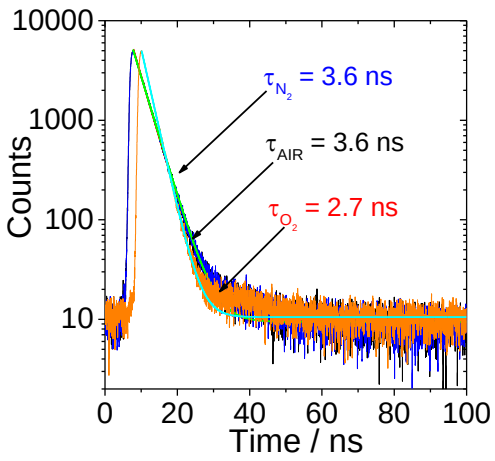


**Fig. S5** Fluorescence decay curves of **BDP-1** in DCM under nitrogen ($N_2$), oxygen ($O_2$) and air atmosphere. $c = 1.0 \times 10^{-5}$ M, excited with EPL picosecond pulsed laser ($\lambda_{ex}$ = 510 nm). Detected with TCSPC mode. 20 °C.

**Table S1 The Photophysical Properties of the BDP-1**

| | Solvent | $\lambda_{abs}$ [a] ($\varepsilon$ [b]) | $\lambda_F$ [c] | $\Phi_F$ [d] | $\tau_F$ [e] | $\Phi_\Delta$ [f] | $\Phi_T$ [g] |
|---|---|---|---|---|---|---|---|
| **BDP-1** | HEX | 562 (1.46) | 568 | 0.37 [h]/0.34 [i] | 4.4 | 0.17 [h]/0.24 [i] | 0.41 |
| | TOL | 566 (1.31) | 575 | 0.47 [h]/0.43 [i] | 4.7 | 0.26 [h]/0.31 [i] | 0.41 |
| | DCM | 564 (1.21) | 572 | 0.31 [h]/0.29 [i] | 3.6 | 0.55 [h]/0.59 [i] | 0.56 |
| | ACN | 557 (1.13) | 568 | 0.36 [h]/0.32 [i] | 4.7 | 0.41[h]/0.45 [i] | 0.39 |

[a] $c$ = $1.0 \times 10^{-5}$ M, in nm. [b] Molar absorption coefficient. $\varepsilon$ values are in $10^5$ $M^{-1}$ $cm^{-1}$. [c] Fluorescence emission maxima wavelength, in nm. [d] Absolute fluorescence quantum yield determined by optical integrating sphere, error: ±0.01. [e] Fluorescence lifetime, $\lambda_{ex}$ = 510 nm, in ns, $c$ = $1.0 \times 10^{-5}$ M. [f] Singlet oxygen quantum yield ($\Phi_\Delta$), $Ru(bpy)_3$ as standard ($\Phi_\Delta$ = 0.57 in ACN) when excited into the $S_2$ state. 2,6-diiodobodipy was used as standard ($\Phi_\Delta$ = 0.85 in toluene) when excited into the $S_1$ state. Estimated determination error: ±0.03. [g] Triplet state quantum yield, 2,6-diiodobodipy as standard ($\Phi_T$ = 0.88 in toluene) when excited at $S_0 \rightarrow S_1$ transition. [h] Excited at $S_0 \rightarrow S_1$ transition. [i] Excited at $S_0 \rightarrow S_2$ transition.

**2.0 Singlet Oxygen Quantum Yield.**

Singlet oxygen quantum yields ($\Phi_\Delta$) were determined by relative method using Eq. S1. 1,3-diphenylisobenzofuran (DPBF) was used as $^1O_2$ scavenger.

$$\Phi_{sam} = \Phi_{std}\left(\frac{1-10^{-A_{std}}}{1-10^{-A_{sam}}}\right)\left(\frac{m_{sam}}{m_{std}}\right)\left(\frac{\eta_{sam}}{\eta_{std}}\right)^2 \qquad \text{(Eq. S1)}$$

In the equation, "sam" and "std" represent the sample and standard, respectively. $\Phi$, $A$, $m$ and $\eta$ represent as singlet oxygen quantum yield, absorbance at excitation wavelength, the slope of the change of absorbance of DPBF at 414 nm over photo-irradiation time and refractive index of solvent used for measurement.

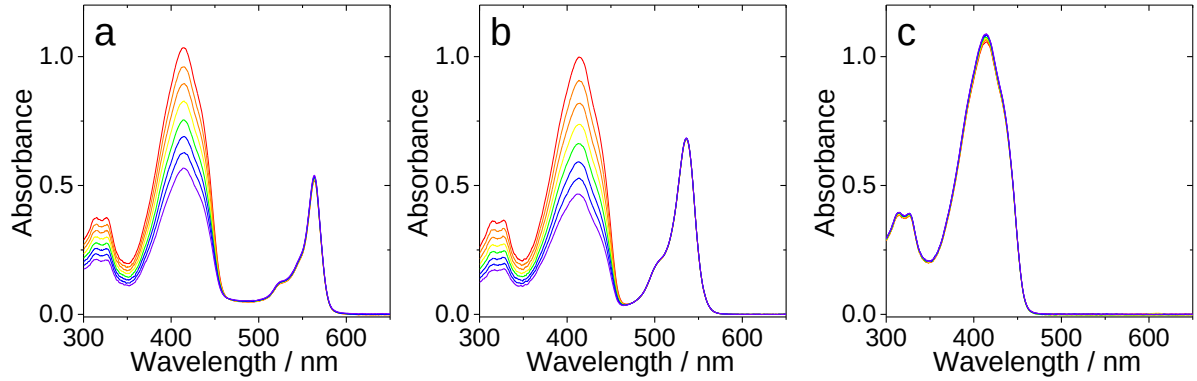


**Fig. S6** Monitoring the $^1O_2$ production using UV–Vis absorption changes of the DPBF upon photo-irradiation with (a) **BDP-1** and DPBF in DCM, (b) **BDP-2** and DPBF in toluene and (c) DPBF in DCM. Optical matched solution was used, $\lambda_{ex} = 550$ nm, the irradiation time for each data point is 20 s (6 mJ cm$^{-2}$). 20 °C.

**3.0 Electrochemical and Spectroelectrochemistry Data.**

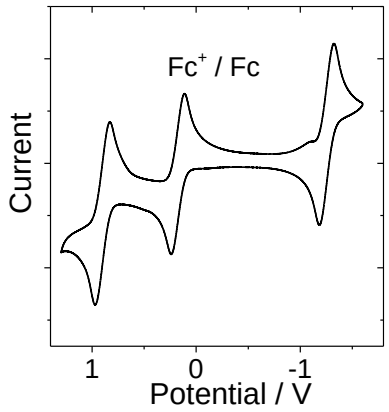


**Fig. S7** Cyclic voltammogram of the **BDP-1**. Ferrocene (Fc) was used as internal reference. In deaerated DCM containing 0.10 M $Bu_4N[PF_6]$ as supporting electrolyte, $Ag/AgNO_3$ as reference electrode. Scan rates: 50 mV/s. $c = 1.0 \times 10^{-3}$ M, 20 °C.

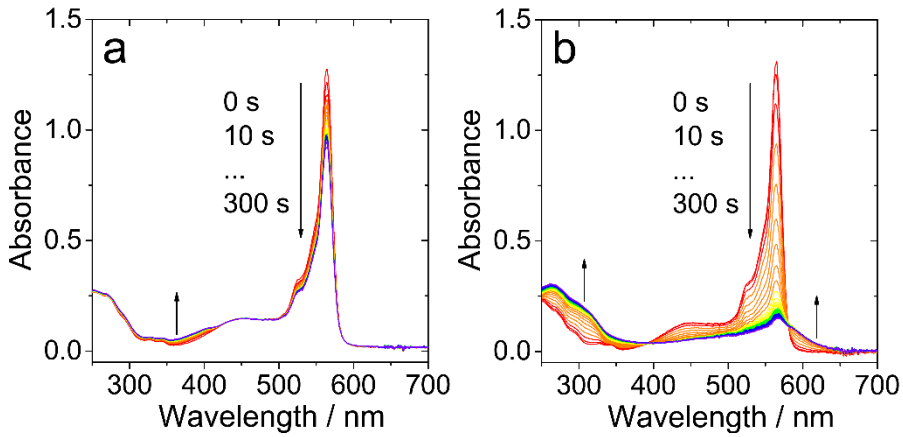


**Fig. S8** Spectroelectrochemistry traces of the UV-Vis absorption spectra observed at controlled-potential. (a) **BDP-1** at −1.17 V and (b) **BDP-1** at +0.95 V. In solution of 0.10 M $Bu_4N[PF_6]$ of DCM. 20 °C.

**4.0 Sub-nanosecond Time-Resolved Transient Absorption Spectra.**

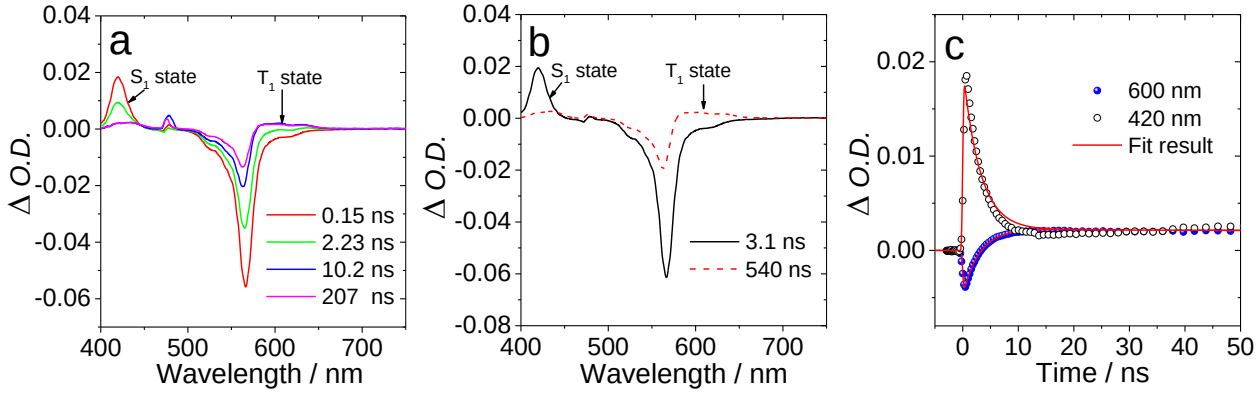


**Fig. S9** Femtosecond transient absorption spectra of **BDP-1**. (a) Transient absorption spectra, (b) Evolution-associated difference spectra (EADS) and (c) Decay traces at selected wavelengths. EADS were obtained by singular value decomposition (SVD) and global fitting (sequential model). $\lambda_{ex}$ = 475 nm, $c = 1.0 \times 10^{-5}$ M in DCM, 20 °C.

**5.0 Nanosecond Time-Resolved Transient Absorption Spectra.**

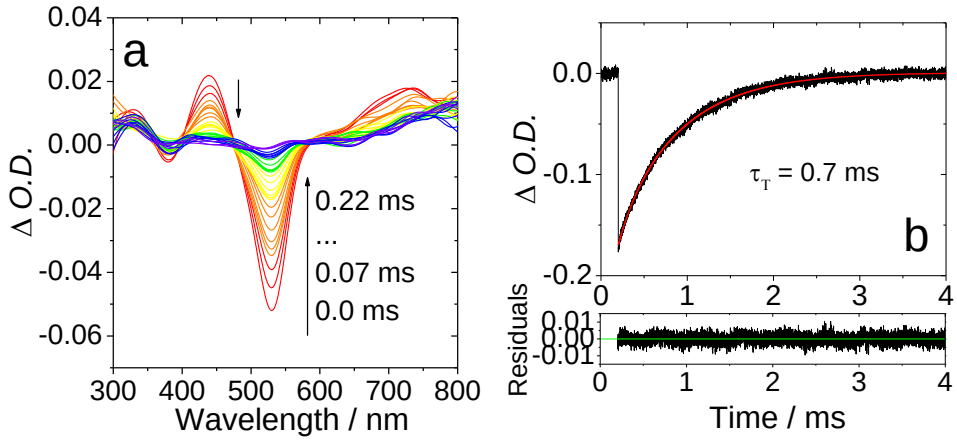


**Fig. S10** (a) Nanosecond transient absorption spectra of **BDP-2** in Clear Flex 50 film under $N_2$ atmosphere. (b) Decay trace at 530 nm. $\lambda_{ex} = 520$ nm, 17.6 μmol/g (**BDP-2**/Clear Flex 50®), 20 °C.

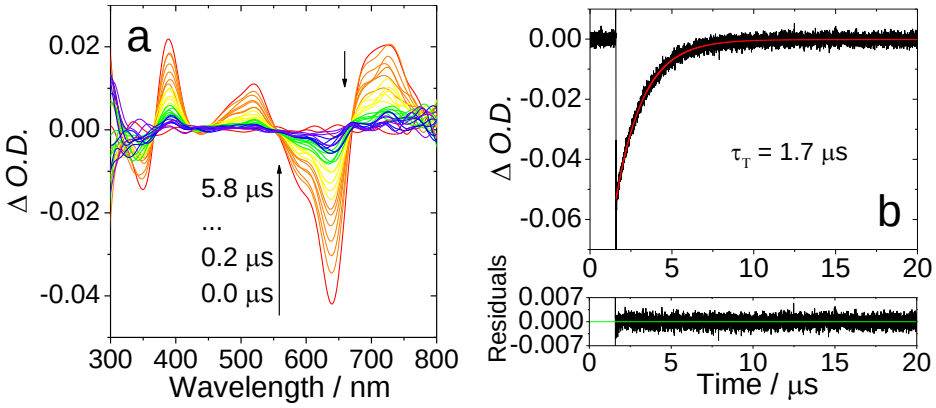


**Fig. S11** (a) Nanosecond transient absorption spectra of **BDP-3** in Clear Flex 50 film under $N_2$ atmosphere. (b) Decay trace at 560 nm. $\lambda_{ex} = 550$ nm, 17.6 μmol/g (**BDP-3**/Clear Flex 50®), 20 °C.

## 6.0 TREPR Spectra of the Triplet State of BDP-1 at Different Delay Times after Laser Flash

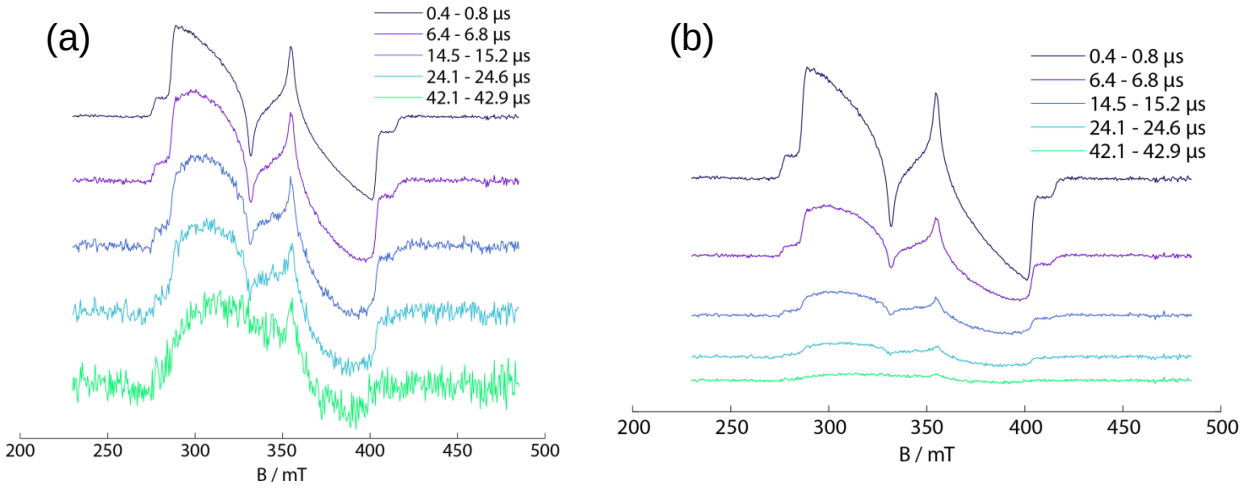


**Fig. S12** The TREPR spectra of **BDP-1** at different delay times after laser flash. (a) Normalized spectra; (b) Original spectra. Recorded by excitation of the frozen solution with 532 nm nanosecond pulsed laser. In toluene/MeTHF (3:1, v/v). 80 K. Integration time window is indicated for each trace.

**7.0 DFT Calculation.**

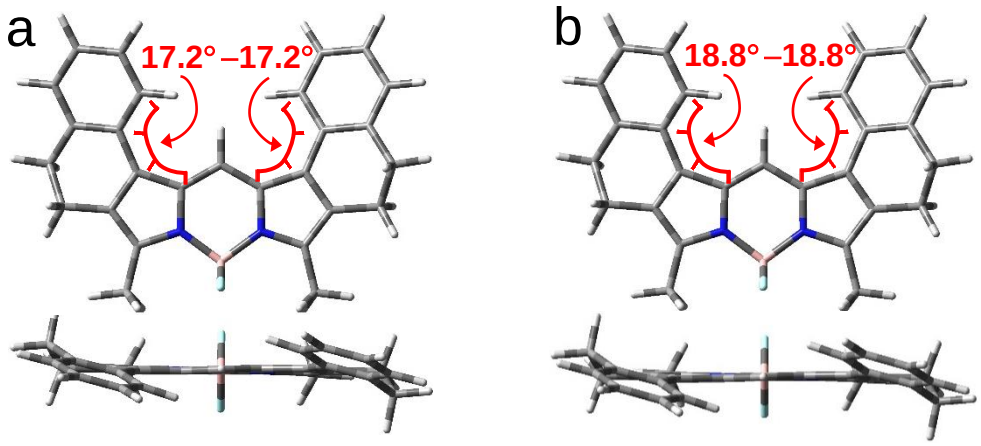


**Fig. S13** Optimized geometries and the dihedral angles of **BDP-1** (a) $S_1$ state and (b) $T_1$ state**.** DFT and TDDFT computation was performed at B3LYP/6-31G(d) level with Gaussian 09W.

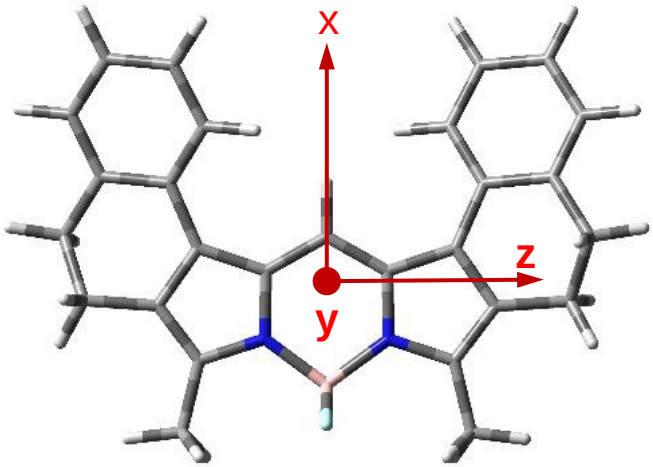


**Table S2. X, Y and Z components of the computed SOC matrix elements of BDP-1**

| Involved excited states | X-component ($cm^{-1}$) | Y-component ($cm^{-1}$) | Z-component ($cm^{-1}$) | Total [a] ($cm^{-1}$) |
|---|---|---|---|---|
| $S_1$-$T_1$ | 0.03 | –0.40 | 0.22 | 0.45749 |
| $S_1$-$T_2$ | –0.08 | –0.13 | 0.02 | 0.15394 |
| $S_1$-$T_3$ | 0.02 | 1.96 | –0.13 | 1.96441 |
| $S_2$-$T_1$ | 0.04 | –0.42 | 0.19 | 0.46271 |
| $S_2$-$T_2$ | 0.03 | 0.47 | –0.15 | 0.49427 |
| $S_2$-$T_3$ | 0.05 | 0.66 | 0.14 | 0.67654 |

[a] Formula used to calculate total SOC from its components is $Total = \sqrt{x^2 + y^2 + z^2}$

**8.0 Application in Photodynamic Therapy**

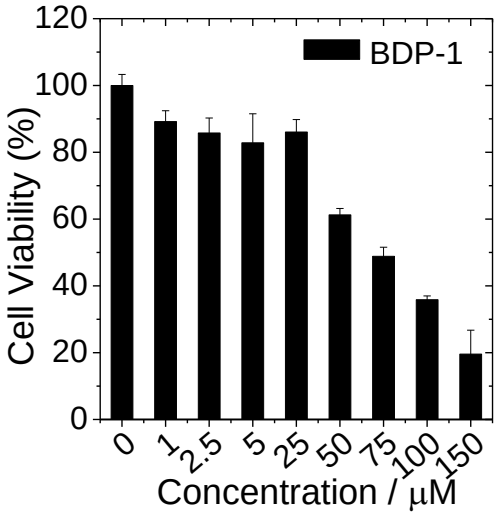


**Fig. S14** Comparison of the cell viability of HeLa cells with pre-treated **BDP-1** with different concentration without light irradiation.

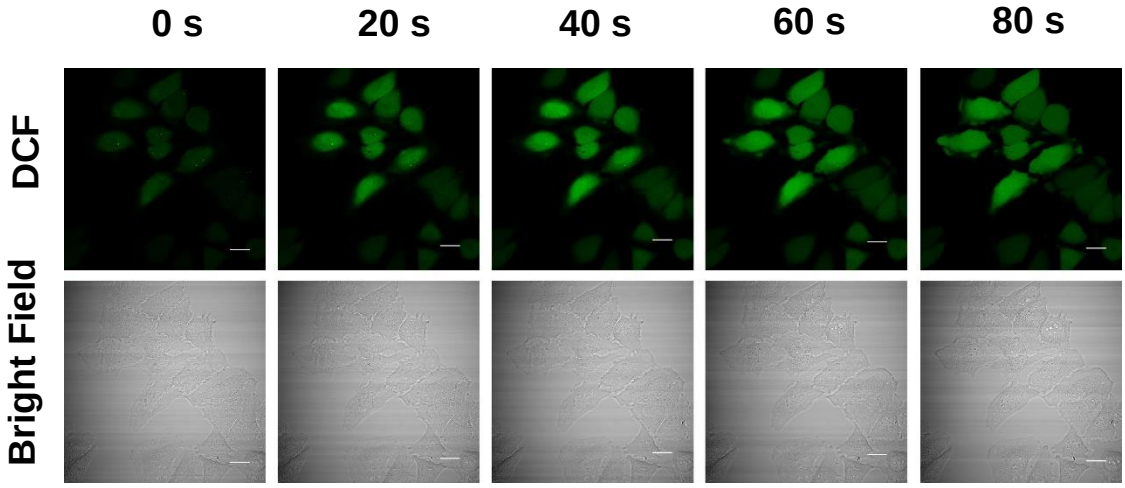


**Fig. S15** Detection of intracellular ROS generation in HeLa cells. The cells were irradiation with 559 nm after incubated with 3 μM **BDP-1** and DCF-DA. The channel of fluorescence image of DCF ($\lambda_{ex}$ = 488 nm; $\lambda_{em}$ = 500–540 nm) and transmitted light images. Scale bar: 20 μm.

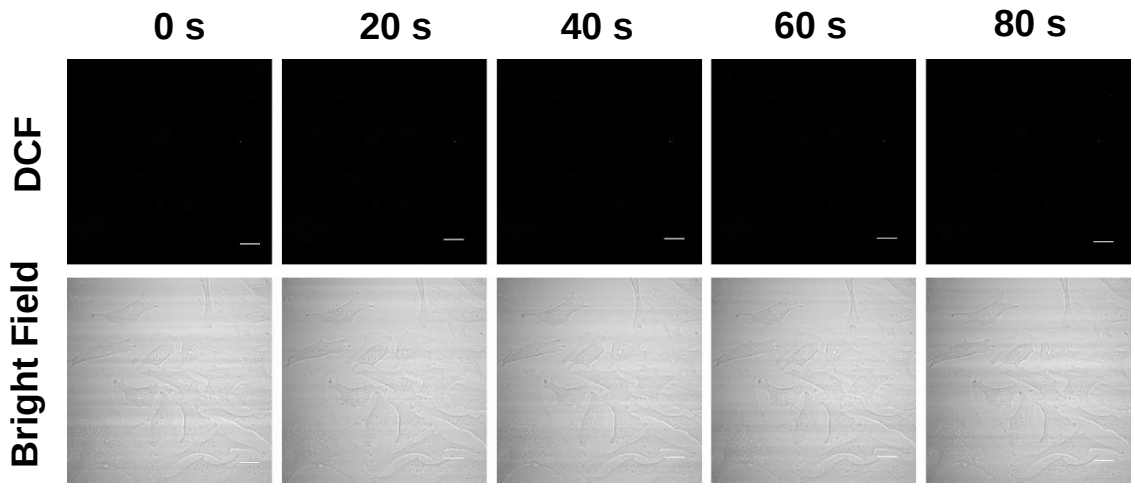


**Fig. S16** Detection of intracellular ROS generation in HeLa cells. The cells were irradiation with 559 nm after incubated with DCF-DA. The channel of fluorescence image of DCF ($\lambda_{ex}$ = 488 nm; $\lambda_{em}$ = 500–540 nm) and transmitted light images. Scale bar: 20 μm.